Thermoresponsive amperometric glucose biosensor

Piyanut Pinyou, Adrian Ruff, Sascha Pöller, Stefan Barwe, Michaela Nebel, Natalia Guerrero Alburquerque, Erik Wischerhoff, André Laschewsky, Sebastian Schmaderer, Jan Szeponik, Nicolas Plumeré, and Wolfgang Schuhmann

Citation: Biointerphases **11**, 011001 (2016); doi: 10.1116/1.4938382

View online: http://dx.doi.org/10.1116/1.4938382

View Table of Contents: http://avs.scitation.org/toc/bip/11/1

Published by the American Vacuum Society

Thermoresponsive amperometric glucose biosensor

Piyanut Pinyou, Adrian Ruff, Sascha Pöller, Stefan Barwe, and Michaela Nebel
Analytical Chemistry - Center for Electrochemical Sciences (CES), Ruhr-Universität Bochum, Universitätsstr. 150, D-44780 Bochum, Germany

Natalia Guerrero Alburquerque and Erik Wischerhoff
Fraunhofer Institute for Applied Polymer Research, Geiselbergstrasse 69, D-14476 Potsdam-Golm, Germany

André Laschewsky
Institut für Chemie, Universität Potsdam, Karl-Liebknecht-Str. 24-25, D-14476 Potsdam-Golm, Germany

Sebastian Schmaderer and Jan Szeponik
BST BioSensor Technology GmbH, Buchholzer Str. 58, D-13156 Berlin, Germany

Nicolas Plumeré
Center for Electrochemical Sciences (CES) - Molecular Nanostructures, Ruhr-Universität Bochum, Universitätsstr. 150, D-44780 Bochum, Germany

Wolfgang Schuhmann[a)]
Analytical Chemistry - Center for Electrochemical Sciences (CES), Ruhr-Universität Bochum, Universitätsstr. 150, D-44780 Bochum, Germany

(Received 3 November 2015; accepted 9 December 2015; published 24 December 2015)

The authors report on the fabrication of a thermoresponsive biosensor for the amperometric detection of glucose. Screen printed electrodes with heatable gold working electrodes were modified by a thermoresponsive statistical copolymer [polymer I: poly(ω-ethoxytriethylenglycol methacrylate-*co*-3-(*N*,*N*-dimethyl-*N*-2-methacryloyloxyethyl ammonio) propanesulfonate-*co*-ω-butoxydiethylenglycol methacrylate-*co*-2-(4-benzoyl-phenoxy)ethyl methacrylate)] with a lower critical solution temperature of around 28 °C in aqueous solution via electrochemically induced codeposition with a *p*H-responsive redox-polymer [polymer II: poly(glycidyl methacrylate-*co*-allyl methacrylate-*co*-poly(ethylene glycol)methacrylate-*co*-butyl acrylate-*co*-2-(dimethylamino)ethyl methacrylate)-[$Os(bpy)_2$(4-(((2-(2-(2-aminoethoxy)ethoxy)ethyl)amino)methyl)-*N*,*N*-dimethylpicolinamide)]$^{2+}$] and pyrroloquinoline quinone-soluble glucose dehydrogenase acting as biological recognition element. Polymer II bears covalently bound Os-complexes that act as redox mediators for shuttling electrons between the enzyme and the electrode surface. Polymer I acts as a temperature triggered immobilization matrix. Probing the catalytic current as a function of the working electrode temperature shows that the activity of the biosensor is dramatically reduced above the phase transition temperature of polymer I. Thus, the local modulation of the temperature at the interphase between the electrode and the bioactive layer allows switching the biosensor from an on- to an off-state without heating of the surrounding analyte solution. © *2015 American Vacuum Society*. [http://dx.doi.org/10.1116/1.4938382]

I. INTRODUCTION

During the last years, stimuli-responsive polymers were widely used in biomedical[1] or analytical[2] applications. The use of such *smart* materials in electrochemical based biosensors enables to tune the properties of the device with respect to the modulation of the electron transfer reaction,[3] the overall biocatalytic process and/or enzyme–electrode interactions.[4–6] Moreover, the activity of the biosensor can be controlled by the degree of swelling of the polymer layer, which can be modulated by temperature changes.[7] The same electrodes show an increased stability against fouling because adsorption of larger molecules (e.g., albumin) to the electrode surface can be prevented by controlling the mesh size in the polymer layer as a function of the degree of swelling.[7]

Nonionic thermoresponsive polymers are prominent representatives of such stimuli-responsive materials.[8,9] Many of these polymers exhibit a lower critical solution temperature (LCST) in aqueous media.[8,10] When heated above the phase transition temperature, the dissolved polymer precipitates due to a coil-to-globule collapse transition of the polymer structure. Thus, switching of the properties of the system can be easily induced by a temperature change used as external trigger. The LCST depends sensitively on the polymer composition/structure and can be fine-tuned for copolymers by varying the ratio of the incorporated comonomers.[10–12] So far, poly(*N*-isopropylacrylamide) (PNIPAM) based materials that reveal a LCST of around 32 °C have been mostly explored for biomedical applications.[9] Apart from PNIPAM, poly(oligoethyleneoxide-(meth)acrylate) based polymers reveal a similar LCST, but have been demonstrated to exhibit improved biocompatibility (see Ref. 8 and references cited therein). Moreover, the thermoresponsive properties of

a)Electronic mail: wolfgang.schuhmann@rub.de

such polymers remain unchanged, even when the polymer is deposited on an electrode surface.[13]

Heatable electrodes are of particular interest for the fabrication of electrochemical biosensors. The change of the temperature leads to altered electron transfer kinetics,[14] changes in mass transport to the electrode surface (*Soret* effect),[15] and can suppress side reactions, like the oxidation of ascorbic acid.[16] Biosensors based on such electrodes exhibit high sensitivities and high specificities for various analytes.[17–19] Recently, we reported on screen printed electrodes that allow for a local heating of only the working electrode by a heating resistance mounted on the back of the aluminum oxide ceramic base of the electrode. A scanning electrochemical microscope (SECM) was used to evaluate the temperature gradient in front of such a heatable electrode by measuring the open-circuit potential of a redox probe at the SECM tip (thermal probe) in close proximity to the heated surface.[20] These electrodes allow for a local temperature modulation at the interphase between the (modified) electrode surface and surrounding electrolyte solution that contains the analyte.

Here, we report on the fabrication of a temperature-triggered glucose biosensor based on locally heatable screen printed (HSP) electrodes and a thermoresponsive polymer. The biosensor was prepared in a codeposition process with the thermoresponsive polymer, a redox-polymer bearing Os-complexes acting as redox mediators, and a biorecognition element.

II. EXPERIMENT

A. Chemicals and reagents

All chemicals and solvents were purchased from Sigma-Aldrich, Alfa Aesar, VWR, J.T. Baker, Fluka or Acros Organics and were used without further purification unless otherwise noted. 4-(2-hydroxyethyl)–1–piperazine ethane sulfonic acid (HEPES), Triton X-100, and D-(+)-glucose monohydrate were purchased from Applichem (Darmstadt, Germany). The apoenzyme soluble glucose dehydrogenase (sGDH) was a gift from Roche Diagnostics (Penzberg, Germany). Pyrroloquinoline quinone (PQQ) was obtained from Fluka (Buchs, Switzerland).

HEPES buffer solution (10 mM, pH = 7) containing 0.1 vol. % Triton-X-100 was prepared by using deionized water (Milli-Q-System). The pH value of the HEPES buffer was adjusted to pH = 7 by adding solid NaOH.

The PQQ-sGDH holoenzyme was reconstituted by adding appropriate amounts of sGDH to a HEPES buffer solution containing PQQ (500 μM) and $CaCl_2$ (150 mM). The final holoenzyme concentration was 24 mg ml^{-1}. The mixture was incubated for approximately 30 min at 4 °C prior to electrode preparation.

B. Synthesis

The synthesis of the redox-polymer P024-P195 [polymer II, poly(glycidyl methacrylate-*co*-allyl methacrylate-*co*-poly(ethylene glycol)methacrylate-*co*-butyl acrylate-*co*–2-(dimethylamino)ethyl methacrylate)-[Os(bpy)$_2$(4-(((2-(2-(2-aminoethoxy)ethoxy)ethyl)amino)methyl)-*N*,*N*-dimethylpicolinamide)]$^{2+}$] was performed as described previously in Ref. 21. It was stored as a polymer suspension in water (2 wt. %). The redox potential of polymer II is ≈0 V vs Ag/AgCl/3 M KCl.[21] The synthesis of the protected crosslinker 2, 2′-(ethylenedioxy)-bis-(*S*-acetylethanthiol) was carried out following the procedure reported in Ref. 22. For the electrochemical preparation of the enzyme electrodes, a 0.1 M solution in dimethyl sulfoxide (DMSO) was used. The structure of all polymers and their nominal compositions are depicted in Fig. 1(a). The synthesis of the 2-(4-benzoylphenoxy)ethyl methacrylate (BPEM) monomer was recently described in Ref. 23.

Synthesis of polymer I–NG017 [poly(ω-ethoxytriethylenglycol methacrylate-*co*-3-(*N*,*N*-dimethyl-*N*-2-methacryloyloxyethyl ammonio) propanesulfonate-*co*-ω-butoxydiethylenglycol methacrylate-*co*-2-(4-benzoyl-phenoxy)ethyl methacrylate)].

The synthesis of NG017 was carried out in the dark, to avoid unintended crosslinking during the free-radical induced polymerization process. The monomers ω-ethoxytriethylenglycol methacrylate (1.540 g, 6.26 mmol, 78 mol. %, inhibitor-free), 3-(*N*,*N*-dimethyl-*N*-2-methacryloyloxyethyl ammonio) propanesulfonate (0.360 g, 1.29 mmol, 16 mol. %), ω-butoxydiethylenglycol methacrylate (0.098 g, 0.43 mmol, 5.4 mol. %, inhibitor-free), and photo cross-linker BPEM (0.016 g, 0.05 mmol 0.6 mol. %) were dissolved in 50 vol. % aqueous ethanol (25 ml). Then, the radical initiator 4,4′-Azobis(4-cyanovaleric acid) (V-501, 8.9 mg, 0.03 mmol) was added, and the reaction mixture was deaerated by argon bubbling for 15 min. The copolymerization was initiated by heating the mixture to 65 °C. After 2 days of stirring at 65 °C, the solvent was evaporated, and the residue was purified by dialysis for 3 days against water (molecular cut-off of the membrane: 4000–6000 kDa). Finally, the product was collected by a freeze-drying to yield 1.68 g (84%) of colorless copolymer. ^{1}H-NMR (D_2O) δ/ppm: broad multiple signals between 0.5 and 2.5 (polymer backbone and -CH_3 groups), broad multiple signals between 2.7 and 5 (-OCH_2CH_2O-groups, -CH_2- of polymer side chains), 7–8 (multiple signals, weak, aromatic protons of the benzophenone core). Size exclusion chromatography (in 0.2% LiBr/dimethyl formamide, 2.1 g·l^{-1}). M_w = 284 kDa, M_n = 87 kDa, and polydispersity index PDI = 3.26. Turbidity measurement revealed a cloud point of 29.5 °C in pure water, and of 28.0 °C in phosphate buffered saline (PBS) buffer.

C. Electrochemical experiments

1. Voltammetric and amperometric experiments

All voltammetric and amperometric experiments were performed with a Gamry 600 potentiostat (Gamry, PA, USA) using a three electrode system screen printed on an alumina oxide ceramic [see below and Fig. 1(b)]. All experiments were conducted in deaerated (argon bubbling) HEPES buffer (10 mM, pH = 7) at the respective temperature (see

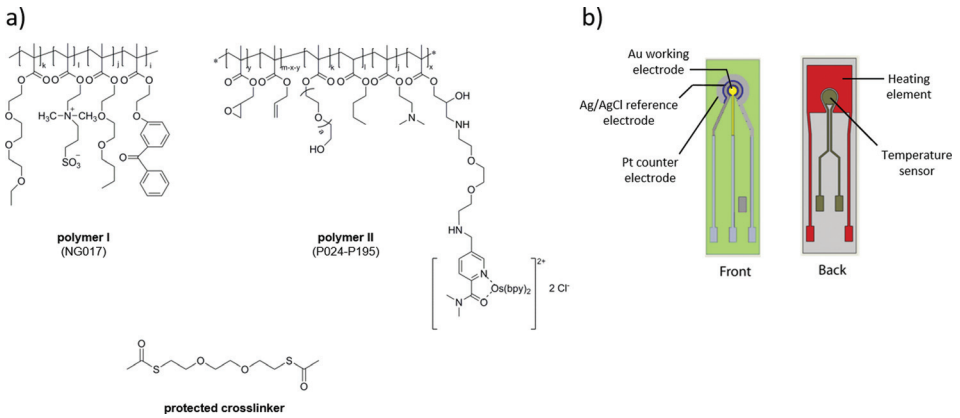

FIG. 1. (a) Proposed structures of the thermoresponsive polymer I (NG017, for synthesis, see Sec. II) and redox-polymer II (P024-P195) (Ref. 21) as well as the molecular structure of the protected dithiol based crosslinker; nominal composition (in mol. %) of the polymer backbones: NG017: k = 78, l = 16, j = 5.4, i = 0.6; PO24-P195: m = 50, k = 7.5, l = 22.5, and j = 20; (b) schematic sketch of the HSP electrodes; the substrate is an aluminum oxide ceramic; electrodes were printed on the front side, thermoelements (heating element and temperature sensor) are located on the back.

main text). For the immobilization of the pristine thermoresponsive polymer, the surface of the gold working electrode was first modified with a cysteamine layer by immersing the electrode into an ethanol solution containing 10 mM of the thiol-amine. After rinsing the electrodes with water, the polymer was drop-coated onto the modified gold electrode and irradiated with UV-light (254 nm) for 10 min.

2. HSP electrodes

Figure 1(b) shows a schematic sketch of the HSP electrodes (BST; prod. code 121100000). The working electrode consisted of a gold disk (nominal diameter = 1.14 mm). The counter electrode was Pt. The pseudoreference electrode was an Ag/AgCl system. The temperature on the working electrode surface was precisely regulated using a proportional-integral-derivative controller (ThermoTrend, BST). The electrodes were electrochemically cleaned by cycling a potential window of 0 to 1.5 V (vs Ag/AgCl 3 M KCl) in 0.5 M H_2SO_4 with a scan rate of 0.1 V s^{-1} (10 cycles). A more detailed description of the electrodes and procedures for the temperature calibration can be found in Ref. 20.

3. Enzyme electrodes

The electrochemical induced codeposition of the thermoresponsive polymer I, PQQ-sGDH, and the redox-polymer II was conducted in a two electrode thin layer Teflon cell with a stainless steel plate acting as the counter and pseudoreference electrode. The bare screen printed electrodes (without cysteamine layer) were inserted directly into the cell which was filled with 100 μl of a electrolyte solution prepared from 50 μl of PQQ-sGDH dissolved in HEPES buffer, 333 μl of the *p*H-sensitive redox-polymer II dissolved in water (2 wt. %), 90 μl of the thermoresponsive polymer I dissolved in water (10 mg ml^{-1}), and 50 μl of a 0.1 M solution of the protected crosslinker in DMSO. For the electrodeposition and the electrochemical induced crosslinking (via the *in situ* deprotection of the acetate protected dithiol crosslinker), the following potential pulse profile was applied: −2.5 V/0.2 s; −0.2 V/1 s; 0 V/5 s; 70 repetitions. After the deposition process, the modified gold electrodes were carefully rinsed with HEPES buffer.

III. RESULTS AND DISCUSSION

A. Thermoresponsive polymer I deposited onto heatable screen printed electrodes

The thermoresponsive polymer I [Fig. 1(a)], which was prepared by a free radical polymerization, exhibits a cloud point of 28 °C (derived from turbidity measurements in PBS, see Sec. II). At this temperature, the polymer switches from a highly hydrated to a more dehydrated state, and undergoes a coil-to-globule conformational collapse in solution, and a volume phase transition in microgels and hydrogel films, respectively. Electrodes that were modified with such stimuli-responsive polymers show different redox behavior of redox probes at temperatures below and above the phase transition.[4,5] Thus, we first investigated the effect of the immobilized polymer I on the redox behavior of a freely diffusing redox probe, i.e., the $[Fe(CN)_6]^{4-}/[Fe(CN)_6]^{3-}$ redox system, at different temperatures.

For a stable anchoring of polymer I, the gold electrodes were first modified with a cysteamine layer prior to the drop cast process. The amino groups of the cysteamine layer can react with the carbonyl groups in the benzophenone core to form imino functions leading to grafting of the polymer film to the cysteamine modified electrode surface by the formation of covalent bonds. In addition, the electrodes were irradiated with UV-light to induce photochemical crosslinking initiated by remaining benzophenone units.[23,24] Under UV-irradiation, benzophenones form radicals that are able to react with alkyl chains[25] within the polymer[26,27] (and/or with the cysteamine layer on the electrode), which leads to a covalent crosslinking. Polymer films that were prepared following this protocol show enhanced stability on the electrode surface. In case of the bare gold electrodes, no stable film formation was observed. Obviously, the premodification of the electrode surface with a cysteamine layer is essential.

It should be noted that stable polymer films can be obtained alternatively by electrostatic interactions between the positively charged ammonium groups located in the polymer side chains and electrode surfaces decorated with negatively charged carboxylates, as it was demonstrated for a similar thermoresponsive polymer.[13] Hence, protonated amine groups of the cysteamine layer, which may be present to some extent in an aqueous electrolyte, may also interact with the sulfonate groups of the polymer and thus contribute to film stability.

Cyclic voltammograms of the redox system $[Fe(CN)_6]^{4-}/[Fe(CN)_6]^{3-}$ in 0.1 M KCl/water at gold electrodes modified with polymer I recorded at 23 °C show a chemically reversible redox couple [Fig. 2(a), blue line] with a rather large peak separation (ΔE_p) of about 350 mV [Fig. 2(b)]. We attribute this effect to a hindered electron transfer reaction most likely because of a slow diffusion (rate limiting step) of the redox probe within the swollen polymer film. The same effect was observed for gold electrodes modified with a similar thermoresponsive polymer.[13] The peak separation of the $[Fe(CN)_6]^{4-}/[Fe(CN)_6]^{3-}$ system at a bare gold electrode is considerably smaller [79 mV, Fig. 2(b), black squares]. By increasing the temperature from 23 to 35 °C [Fig. 2(a), red line], values for ΔE_p decrease [Fig. 2(b), red filled circles]. Simultaneously, the absolute peak currents for the oxidation (I_p^{ox}) and reduction (I_p^{red}) increase [Figs. 2(c) and 2(d), red filled circles]. In contrast, values for ΔE_p and the peak currents at a bare gold electrode remain almost constant over the whole temperature range [Figs. 2(b)–2(d), black squares]. The increase in the current response and the faster kinetics when going from 23 to 28 °C are attributed to a faster diffusion of the redox probe within the film and thus to a faster overall electron transfer reaction. At temperatures above the phase transition of the polymer (>28 °C) changes in ΔE_p and the peak currents are rather small. At these elevated temperatures, the polymer coil collapses and forms a dense and hydrophobic layer on the electrode surface, which hinders the charged redox probe from diffusing to the electrode surface (the increase in current with increasing temperature becomes smaller). Obviously, the LCST properties of the polymer are not affected, even in the immobilized state. It should be noted that for other stimuli-responsive polymers, a complete blocking of the electrode surface was observed when exceeding the phase transition temperature.[28]

The overall higher peak currents in the case of the polymer modified electrodes are striking. The enhanced current values, compared to those that were observed for the bare electrode, may be attributed to an accumulation/entrapment of the redox species within the film and/or to a transition from a diffusion controlled process [$I_p \sim$ (scan rate)$^{1/2}$, large ΔE_p] at low temperatures to a more adsorption controlled process ($I_p \sim$scan rate, small ΔE_p) at high temperatures

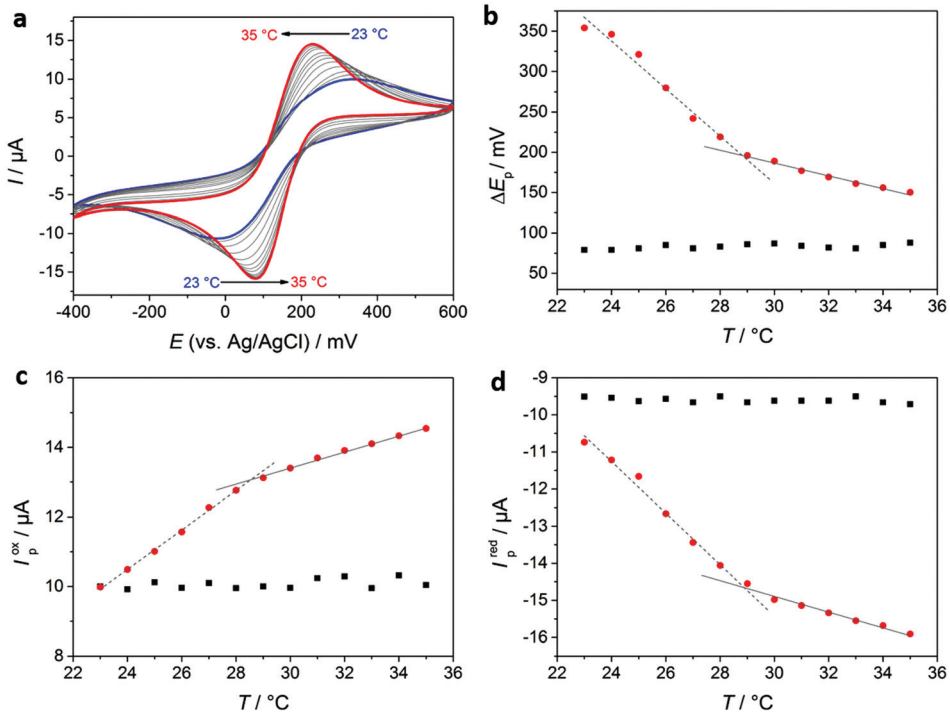

FIG. 2. Voltammetric characterization of the $[Fe(CN)_6]^{4-}/[Fe(CN)_6]^{3-}$ redox system (overall concentration = 5 mM, 1:1 ratio) in 0.1 M KCl/water at different temperatures at a HSP electrode modified with polymer I [(a) and (b)–(d): red filled circles] and a bare HSP electrode [(b)–(d): black squares]. (a) Cyclic voltammograms in the temperature range of 23–35 °C recorded with a scan rate of 0.1 V s^{-1} (10th cycle); blue and red lines: voltammograms recorded at 23 and 35 °C, respectively; gray lines voltammograms in the range of 24–34 °C; (b) plot of the peak separation potential ΔE_p vs the temperature, dotted line: linear fit of the data between 23 and 28 °C, $R^2 = 0.9631$, solid line: linear fit of the data between 29 and 35 °C, $R^2 = 0.9820$; (c) and (d) plots of the absolute peak currents for the oxidation (c) and reduction (d) as a function of temperature; dashed lines: fit of the data between 23 and 28 °C [(c): $R^2 = 0.9987$, (d): $R^2 = 0.9812$], solid lines: linear fit of the data between 29 and 35 °C [(c): $R^2 = 0.9974$, (d): $R^2 = 0.9700$].

(entrapped iron species are then in close proximity to the electrode surface).

The intersection of the linear fits in the temperature ranges 23–28 °C (dashed lines) and 29–35 °C (solid lines) are located at 28.8 °C (b, ΔE_p vs T), 28.5 °C (c, I_p^{ox} vs T) and 28.9 °C (d, I_p^{red} vs T). These values are in good agreement with the cloud point of the polymer in solution. Thus, electrochemistry can be used to corroborate data obtained from turbidity measurements. This effect was recently reported in more detail by Lisdat and coworkers for a similar thermoresponsive polymer.[13]

Based on these findings, the fabrication of a temperature triggered biosensor was attempted by the codeposition of an Os-complex modified redox-polymer (polymer II, Fig. 1), the PQQ-sGDH holoenzyme, and the thermoresponsive polymer I. Such electrodes should allow to switch from a well hydrated/active state ($T < \text{LCST}$) to a dehydrated/non-active state ($T > \text{LCST}$). Below the phase transition, the hydrophilic glucose molecules may easily enter the active layer (high glucose concentration in the film): the conversion of the substrate by the enzyme is not hampered by insufficient mass transport. Above the phase transition, the collapsed, dense film prevents a fast diffusion of the substrate into the film, and thus, the glucose concentration in the film is low. Moreover, the selective control of the temperature only at the working electrode, without heating of the surrounding electrolyte solution (i.e., a local temperature change at the interphase between sensor and electrolyte solution), should enable a temperature triggered on/off switch of the biosensor (Fig. 3).

For shuttling the electrons from PQQ-sGDH to the electrode an Os-complex modified redox-polymer with a redox potential of around 0 V vs Ag/AgCl/3 M KCl (Ref. 21) was employed. The low formal potential of this redox polymer ensures low operating potentials of the sensor, and thus, the minimization of unintended side reactions with electroactive interferences, e.g., among others, ascorbic acid or uric acid, which are often present under physiological conditions.[29] Moreover, the polymer backbone bears *p*H-sensitive amino functions. These allow for an electrochemical induced deposition of the polymer by changing the *p*H value in front of the electrode, applying short potential pulses that are high/low enough for the electrolysis of water. The synthesis of polymer II and the biocatalytic activity of this polymer in combination with PQQ-sGDH was reported earlier in Ref. 21.

B. Enzyme electrodes and effect of temperature

Enzyme electrodes based on heatable screen printed electrodes were prepared via an electrochemical induced deposition from aqueous solutions by the local formation of an OH^- gradient in front of the electrode using short potential pulses of −2.5 V (vs Ag/AgCl pseudoreference electrode). The film stability was improved by using a thiol based bifunctional crosslinker (Fig. 3, bottom), which was *in situ* activated by the removal of the acetate protecting groups under basic conditions during the deposition process. The HSP electrodes were modified under two different diffusional conditions: (1) under planar diffusion conditions in a conventional electrochemical cell and (2) under thin layer conditions in a custom-made electrochemical thin layer cell. The concentrations of polymer I and polymer II during the deposition were ≈1.7 and ≈12.8 mg ml^{-1}, respectively. The concentration of PQQ-sGDH during the deposition process was 2.3 mg ml^{-1}.

Biocatalytic activity of the films at 23 °C was tested using chronoamperometry [Fig. 4(a)] in the presence of glucose (12 mM), applying a potential of +50 mV versus the Ag/AgCl pseudoreference electrode [note that the redox potential of polymer II is located at around −180 mV versus the Ag/AgCl pseudoreference system of the HSP electrode, see Fig. 4(b) black line]. The current response from the HSP electrodes modified under planar diffusion conditions [Fig. 4(a), black line] show a rather low catalytic current (≈45 nA) upon the addition of 12 mM glucose. In contrast, electrodes that were modified under thin layer conditions (dashed line) show a pronounced current response (≈180 nA). We attribute the difference to a thinner active layer formed under planar diffusion conditions, because here the mass transport to the electrode is limited by the diffusion

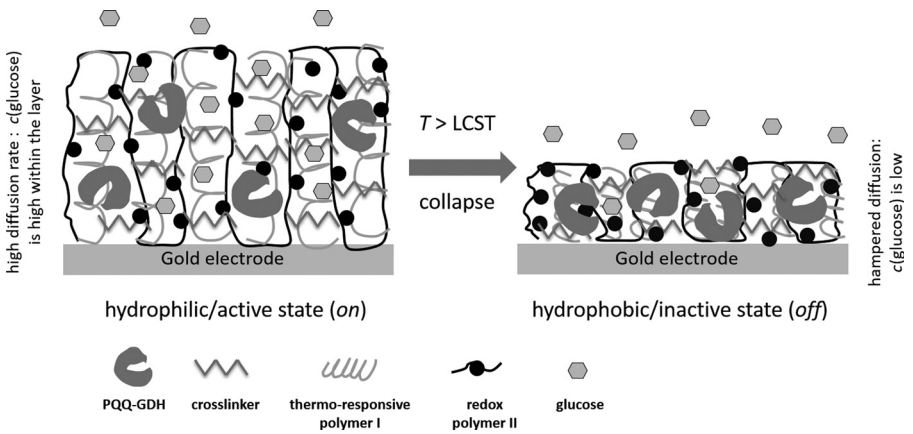

FIG. 3. Schematic representation of the envisaged stimuli-responsive glucose biosensor based on the combination of the thermoresponsive polymer I and the heatable screen printed electrodes.

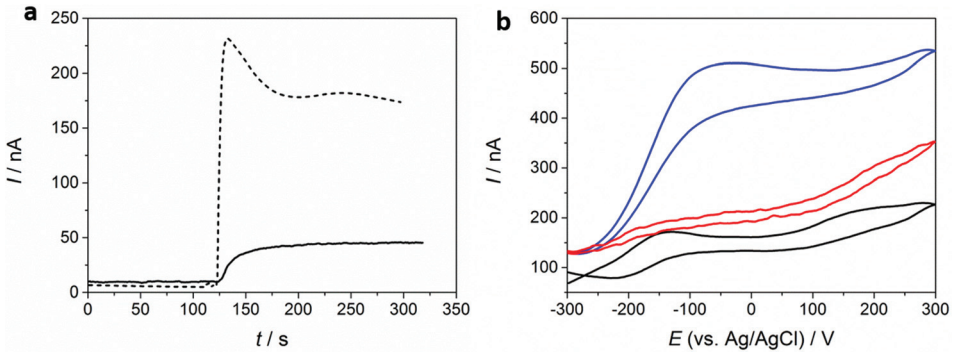

FIG. 4. Amperometric and voltammetric characterization of the enzyme electrodes; (a) chronoamperometric measurements of enzyme electrodes prepared under planar diffusion conditions (solid line) and under thin layer conditions (dashed line), applied potential +50 mV (vs Ag/AgCl pseudoreference) in HEPES buffer (*p*H = 7) with a glucose concentration of 12 mM. (b) Cyclic voltammograms of enzyme electrodes (prepared at 34 °C) in the absence (black line) and presence (red and blue line) of glucose (3 mM) recorded at 23 °C (black and blue curve) and 34 °C (red curve) in HEPES buffer (*p*H = 7), all voltammograms were recorded with a scan rate of 5 mV s^{-1}.

coefficient of the big polymer chains [small diffusion coefficient since $D \sim M^{-1}$ (Refs. 30 and 31)]. Moreover, the steeper OH^- concentration gradient, and thus a higher *p*H value in the diffusion layer within the thin layer cell, may lead to a more efficient deposition of the *p*H-sensitive polymer II and a more efficient deprotection of the thiol groups of the crosslinker. Nevertheless, the *I-t* curves of both electrodes demonstrate that the codeposition of the thermoresponsive polymer I with the redox-polymer II and PQQ-sGDH leads to biocatalytically active films on the electrode surfaces. Moreover, cyclic voltammograms recorded at 23 °C in the absence [Fig. 4(b), black line] and in the presence (blue line) of glucose (3 mM) clearly demonstrate that the extraction of the electrons from the enzyme proceed via the Os-complex modified redox polymer: the onset of the catalytic current (blue curve) overlaps with the redox potential of the Os(II)/Os(III) couple. A direct electron transfer from the enzyme to the electrode can be excluded [note that the redox potential of PQQ-sGDH is at −195 mV vs Ag/AgCl 3 M Cl^- (Refs. 32 and 33)].

Cyclic voltammograms recorded at 34 °C working electrode temperature [Fig. 2(b), red line], above the phase transition of polymer I, show rather low catalytic currents. Obviously, by increasing the temperature above the phase transition of polymer I, the biosensor can be switched to an inactive state. This is in line with our findings in the cyclic voltammetric experiments: the thermoresponsive polymer blocks the surface of the electrode in the collapsed state.

To shed further light on this effect and to identify the temperatures at which the biosensors is *switched off*, chronoamperometric experiments with a glucose concentration of 12 mM and an applied potential of +50 mV at temperatures between 24 and 36 °C were performed. Figure 5 shows the limiting currents extracted from the *I-t* curves as a function of the temperature of the working electrode. A dramatic decrease in the current at temperatures above 27 °C is observed. Despite the codeposition with redox-polymer II and PQQ-sGDH, the thermoresponsive polymer I seems to dominate the film properties on the electrode surface: the enzyme is entrapped in a hydrophobic and dense layer, diffusion of the substrate to the enzyme is tremendously limited. Moreover, the temperature at which the biosensor switches from an "on" to an "off" state (≈27 °C) is close to the cloud point of the pristine polymer. Thus, the codeposition has no significant effect on the phase-transition temperature of polymer I. This is in contrast to other thermoresponsive polymers, where biospecific recognition within the active layer alters their phase transition temperature.[34]

It should be noted that when the temperature is decreased again, only a minor portion of the original catalytic current could be restored. This suggests that the polymer film remains collapsed possibly due to further crosslinking occurring in the collapsed state. Additionally, the PQQ-sGDH or the redox polymer may desorb from the electrode upon the temperature induced phase transition of polymer I. Nevertheless, the codeposition of the thermoresponsive polymer I and the redox-polymer II together with PQQ-sGDH leads to the fabrication of the envisaged temperature triggered biosensor that can be switched from an active on state at low temperatures to an (almost) nonactive off state.

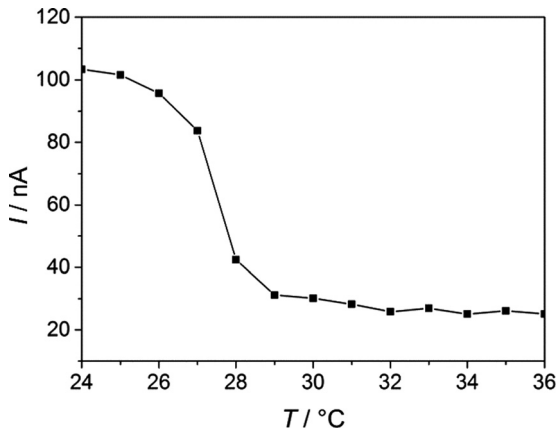

FIG. 5. Effect of temperature on the thermoresponsive biosensor; current values were extracted from chronoamperometric measurements in HEPES buffer (*p*H = 7) with a glucose concentration of 12 mM and an applied potential of +50 mV (vs Ag/AgCl pseudoreference).

IV. SUMMARY AND CONCLUSIONS

A novel thermoresponsive glucose biosensor was successfully fabricated by using heatable screen printed electrodes in combination with a thermoresponsive polymer I (immobilization matrix) that was codeposited with PQQ-sGDH, acting as the biorecognition element, and an Os-complex modified redox-polymer II, acting as the electron relay for shuttling the electrons from the enzyme to the electrode surface. The thermoresponsive properties of polymer I remain intact, even in the bioactive layer. Thus, the local modulation in temperature at the interface between the electrode and the surrounding analyte solution allows switching from an active (*on*) state to a nonactive (*off*) state of the biosensor by increasing the temperature above the phase transition temperature. Such architectures may open new routes for reversible and stable on/off switchable biosensors or biofuel cells.

ACKNOWLEDGMENTS

The authors acknowledge the financial support from the German Federal Ministry of Education and Research (BMBF) initiative "Spitzenforschung & Innovation in den neuen Ländern," within the cooperative project "Das Taschentuchlabor – Impulszentrum für Integrierte Bioanalyse" (03IS2201B/C/F) and the Deutsche Forschungsgemeinschaft (DFG) in the framework of the Cluster of Excellence RESOLV (EXC 1069). P.P. thanks the Deutscher Akademischer Austauschdienst (DAAD) for a Ph.D. fellowship.

[1]A. S. Hoffman, Adv. Drug Delivery Rev. **65**, 10 (2013).
[2]M. R. Islam, Z. Lu, X. Li, A. K. Sarker, L. Hu, P. Choi, X. Li, N. Hakobyan, and M. J. Serpe, Anal. Chim. Acta **789**, 17 (2013).
[3]G. Pelossof, R. Tel-Vered, S. Shimron, and I. Willner, Chem. Sci. **4**, 1137 (2013).
[4]Y. Liang, H. Liu, K. Zhang, and N. Hu, Electrochim. Acta. **60**, 456 (2012).
[5]B. Nagel, A. Warsinke, and M. Katterle, Langmuir **23**, 6807 (2007).
[6]I. Tokarev, M. Orlov, E. Katz, and S. Minko, J. Phys. Chem. B **111**, 12141 (2007).
[7]J. Bünsow, A. Enzenberg, K. Pohl, W. Schuhmann, and D. Johannsmann, Electroanalysis **22**, 978 (2010).
[8]J.-F. Lutz, J. Polym. Sci. A Polym. Chem. **46**, 3459 (2008).
[9]E. Gil and S. Hudson, Prog. Polym. Sci. **29**, 1173 (2004).
[10]J.-F. Lutz, K. Weichenhan, Ö. Akdemir, and A. Hoth, Macromolecules **40**, 2503 (2007).
[11]J. H. Priest, S. L. Murray, R. J. Nelson, and A. S. Hoffman, ACS Symp. Ser. **350**, 255 (1987).
[12]H. Kitano, T. Hirabayashi, M. Gemmei-Ide, and M. Kyogoku, Macromol. Chem. Phys. **205**, 1651 (2004).
[13]A. Fandrich, J. Buller, E. Wischerhoff, A. Laschewsky, and F. Lisdat, ChemPhysChem **13**, 2020 (2012).
[14]J. Wang and P. Gründler, Electroanalysis **15**, 1756 (2003).
[15]S. Duhr and D. Braun, PNAS **103**, 19678 (2006).
[16]C. Lau, S. Reiter, W. Schuhmann, and P. Gründler, Anal. Bioanal. Chem. **379**, 255 (2004).
[17]J.-H. Ke, H.-J. Tseng, C.-T. Hsu, J.-C. Chen, G. Muthuraman, and J.-M. Zen, Sens. Actuators B **130**, 614 (2008).
[18]C. Lau, S. Borgmann, M. Maciejewska, B. Ngounou, P. Gründler, and W. Schuhmann, Biosens. Bioelectron. **22**, 3014 (2007).
[19]T.-F. Tseng, Y.-L. Yang, M.-C. Chuang, S.-L. Lou, M. Galik, G.-U. Flechsig, and J. Wang, Electrochem. Commun. **11**, 1819 (2009).
[20]A. Sode, M. Nebel, P. Pinyou, S. Schmaderer, J. Szeponik, N. Plumeré, and W. Schuhmann, Electroanalysis **25**, 2084 (2013).
[21]P. Pinyou, S. Pöller, X. Chen, and W. Schuhmann, Electroanalysis **27**, 200 (2015).
[22]S. Pöller, D. Koster, and W. Schuhmann, Electrochem. Commun. **34**, 327 (2013).
[23]J. Buller, A. Laschewsky, and E. Wischerhoff, Soft Matter **9**, 929 (2013).
[24]R. S. P. Teixeira, R. J. Correa, A. Belvino, and R. S. V. Nascimento, J. Appl. Polym. Sci. **130**, 2458 (2013).
[25]G. Dorman and G. D. Prestwich, Biochemistry **33**, 5661 (1994).
[26]N. Griep-Raming, M. Karger, and H. Menzel, Langmuir **20**, 11811 (2004).
[27]O. Prucker, C. A. Naumann, J. Rühe, W. Knoll, and C. W. Frank, J. Am. Chem. Soc. **121**, 8766 (1999).
[28]J. Zhou, G. Wang, J. Hu, X. Lu, and J. Li, Chem. Commun. **2006**, 4820.
[29]J. Wang, Chem. Rev. **108**, 814 (2008).
[30]D. P. Valencia and F. J. González, Electrochem. Commun. **13**, 129 (2011).
[31]D. P. Valencia and F. J. González, J. Electroanal. Chem. **681**, 121 (2012).
[32]V. Flexer and N. Mano, Anal. Chem. **86**, 2465 (2014).
[33]A. Sato, K. Takagi, K. Kano, N. Kato, J. A. Duine, and T. Ikeda, Biochem. J. **357**, 893 (2001).
[34]J. Buller, A. Laschewsky, J.-F. Lutz, and E. Wischerhoff, Polym. Chem. **2**, 1486 (2011).